IEEE Photonics Journal
An IEEE Photonics Society Publication

Open Access

Experimental Demonstration of an Indoor VLC Positioning System Based on OFDMA

Volume 9, Number 2, April 2017

Bangjiang Lin
Xuan Tang
Zabih Ghassemlooy, *Senior Member, IEEE*
Chun Lin
Yiwei Li

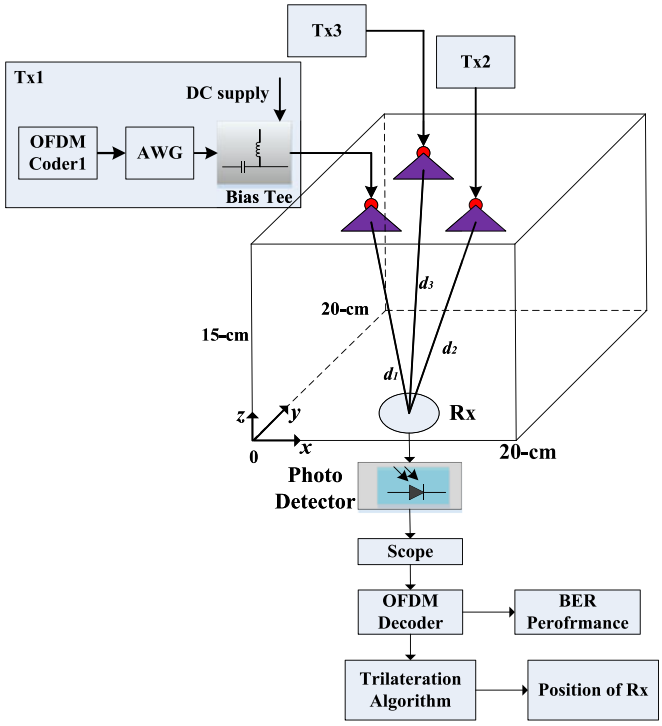

DOI: 10.1109/JPHOT.2017.2672038
1943-0655 © 2017 IEEE

Experimental Demonstration of an Indoor VLC Positioning System Based on OFDMA

Bangjiang Lin,[1] **Xuan Tang,**[1]
Zabih Ghassemlooy,[2] ***Senior Member, IEEE*, Chun Lin,**[1] **and Yiwei Li**[1]

[1]Quanzhou Institute of Equipment Manufacturing, Haixi Institutes, Chinese Academy of Sciences, Quanzhou 362200, China
[2]Optical Communications Research Group, NCRLab, Faculty of Engineering and Environment, Northumbria University, Newcastle NE1 8ST, U.K.

DOI:10.1109/JPHOT.2017.2672038

Manuscript received November 7, 2016; revised January 17, 2017; accepted February 16, 2017. Date of publication February 20, 2017; date of current version March 8, 2017. This work was supported in part by the Chunmiao Project of Haixi Institutes, Chinese Academy of Sciences; in part by the National Science Foundation of China under Grant 61601439 and Grant 61501427; in part by the External Cooperation Program of Chinese Academy of Sciences under Grant 121835KYSB20160006; and in part by the State Key Laboratory of Advanced Optical Communication Systems and Networks, China.
Corresponding author: B. Lin (e-mail: linbangjiang@163.com).

Abstract: We propose an indoor visible light communication (VLC) and positioning system using the orthogonal frequency division multiplexing access (OFDMA) scheme, which can provide both indoor positioning and communications. Three subcarriers with the maximum received signal intensity with respect to three light-emitting diodes (LEDs) are selected for indoor positioning based on the trilateration algorithm. The experiment results show that the proposed system with quadrature phase shift keying (QPSK) mapping offers a mean positioning error and an error vector magnitude of 1.68 cm and more than 15 dB, respectively.

Index Terms: Visible light communication (VLC), orthogonal frequency division multiplexing access (OFDMA), indoor positioning.

1. Introduction

Visible light positioning systems using light-emitting diodes (LED) has been an attractive research topic [1], [2], due to the advantages of high positioning accuracy, license-free operation, no radio frequency (RF) interference, low-cost front-ends, etc. The indoor positioning methods based on visible light communications (VLC) are mainly as follows: triangulation based on received signal strength (RSS), fingerprints analysis, proximity, and image positioning method. The proximity method is very simple but provides accuracy no more than the resolution of the grid itself [3]. In fingerprints analysis based method the target's location is determined by matching real-time measurements with the fingerprints data base [4]. The disadvantage of this scheme is that it will result in inaccurate positioning because of the changes in the environment and the fingerprints data base not being updated. The image positioning method can measure both the receiver's position and direction in indoor environment with high accuracy [5]. However, it requires additional image processing techniques for wireless communications and the data rate is dependent on the image processing speed. The triangulation method estimates the transmission distance via received signal strength

(RSS) based on the intensity modulation and direct detection (IM/DD) [6]. In public indoor places with a large number of LEDs for lighting, the coverage area of LEDs will overlaps, thus resulting in intercell interference (ICI). To overcome this problem, a number of schemes including carrier allocation, time allocation, and wavelength allocation have been investigated. Both time and wavelength allocation based techniques will require synchronization and optical filtering or multiple receivers [7]–[9]. Whereas, in the carrier allocation scheme, many radio frequecncy (RF) based filters needs integration in a single receiver (Rx), which is not applicable in an indoor environment with numerous LEDs [6].

In this paper, we propose an indoor VLC and positioning system using the orthogonal frequency division multiplexing access (OFDMA) scheme, in which the signals transmitted by LEDs are encoded with allocated subcarrier, respectively and the Rx recovers all transmitted signals using a discrete Fourier transformation (DFT) operation. Three subcarriers, with the maximum received signal intensity with respect to three LEDs, are selected for indoor positioning. The proposed indoor positioning system can measure the receiver's position with not ICI as well as providing data communications. The feasibility of the scheme is demonstrated in a room of size 20 $\times$ 20 $\times$ 15 cm. We show that the proposed scheme offers a mean positioning error (PE) of 1.68 cm and the error vector magnitude (EVM) is more than 15 dB for a $\sim$20 cm free space transmission span.

The rest of the paper is organized as follow: Section 2 describes the proposed indoor positioning scheme in detail. Section 3 presents the experiment setup and results for OFDMA-VLC positioning system followed by the concluding remarks in Section 4.

2. Proposed System for Indoor Positioning

Fig. 1(a) shows the block of proposed scheme with an LED grid. We assume LEDs are distributed evenly on the ceiling of a large hall. In order to acquire the position of receiver (Rx), different position information should be transmitted from the respective LEDs. Since the illuminated LEDs are densely arranged, ICI is a serious problem for a large indoor environment. In this paper, in order to receive the information correctly, signals transmitted from LEDs are encoded with dedicated subcarrier frequencies f_i, where $i = 1, 2, 3 \ldots L$. L is the number of LEDs as shown in Fig. 1(a). Out of the total number of N-subcarriers L-subcarrier are used for indoor positioning and N-L subcarriers are reserved for broadcasting information. Since OFDMA can be regarded as a special means of carrier allocation, the frequency reuse method proposed in [10] can also be applied for OFDMA-VLC positioning systems. When frequency reuse method is deployed, the total number of subcarriers can be far less than the number of LEDs. As shown in Fig. 1(b) the emitted signal from the i-th LED transmitter (Tx_i) following an inverse discrete Fourier transformation (IDFT) can be expressed as

$$S_i(t) = A\cos(2\pi i \Delta f t + \alpha_i) \tag{1}$$

where Δf is the frequency spacing of adjacent subcarriers, A is the amplitude of the transmitted signal, and α_i is the phase of modulated signal. Due to the similar characteristic between visible light and infrared [11], the channel gain H_i of Tx_i and Rx is given by

$$H_i = \begin{cases} \frac{A_r(m+1)}{2\pi d_i^2}\cos^m(\varphi_i) T_s G_s \cos(\phi_i), & 0 \le \phi_i \le \phi_c \\ 0, & \phi_i > \phi_c \end{cases} \tag{2}$$

where m is the order of Lambertian emission, which is relative to the semi-angle at half illuminance of the LED denoted as $\varphi_{1/2}$, and is defined as

$$m = -\ln 2 / \ln(\cos(\varphi_{1/2})). \tag{3}$$

A_r is the physical area of the detector, d_i is the distance between the Tx_i and the Rx, and φ_i and ϕ_i are the angles of irradiance and incidence, respectively. ϕ_c denotes the field of view (FOV) of the Rx, T_s is the gain of the optical filter, and G_s is the gain of the optical concentrator, which is given

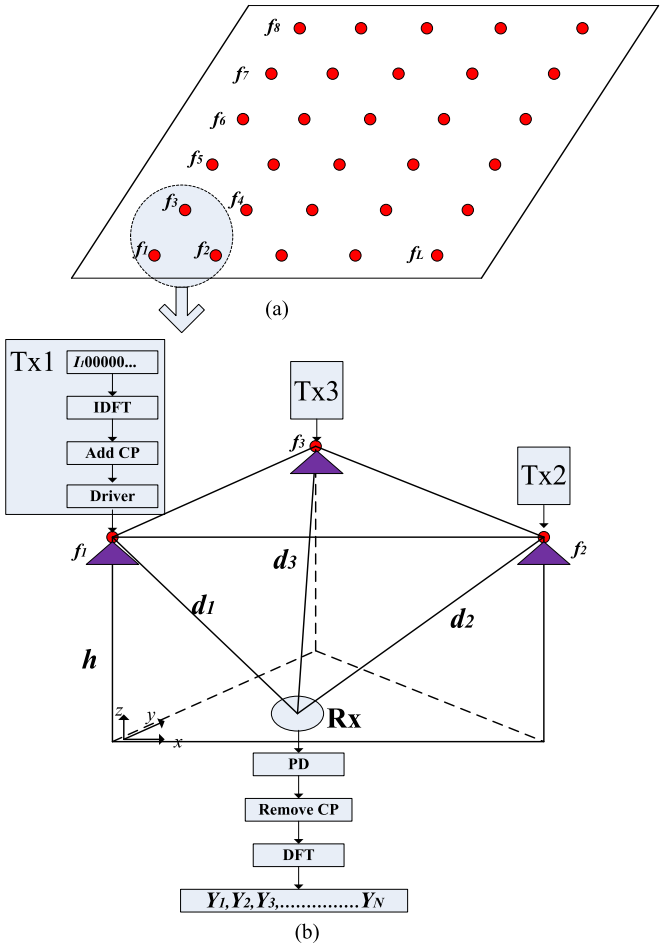

Fig. 1. (a) Block of LEDs in the proposed scheme and (b) the basic unit and the structures of transmitter and receiver.

by

$$G_s = \begin{cases} \frac{n^2}{\sin^2(\phi_c)}, & 0 \le \phi_i \le \phi_c \\ 0, & \phi_i \ge \phi_c \end{cases} \tag{4}$$

where n denotes the refractive index. In VLC, the influence of the directed light is large and greatly depends on the performance of the system [11]; therefore, only the line of sight (LOS) link is considered in this work. Note that within a typical indoor optical illumination footprint delay spread due to multipath will be very small, and therefore can be ignored. However, the channel characteristics can change due to movement of people (i.e., shadowing) that can lead to temporarily link blockage [12]. To address this problem and therefore enhance the user's mobility multiple Rxs have been used as in [13].

In view of the influence of noise (mostly the ambient and natural light), the received signals can be expressed as

$$y(t) = R \times \sum H_i \times S_i(t) + n(t) \tag{5}$$

where R is the Rx responsivity, and $n(t)$ is the noise. At the Rx the invers of Tx is adopted (i.e., DFT operation) to recover the signal. For the i-th subcarrier, the received signal is given as

$$Y_i = R \times H_i \times A + N_i \tag{6}$$

where N_i is the noise term expressed in the frequency domain. Then, the three subcarriers with the maximum received signal intensity with respect to three LED Txs are selected for indoor positioning. The basic unit for trilateration positioning is shown in Fig. 1(b). Provided the Rx is within the triangle areas, see Fig. 1(b), Y_1, Y_2 and Y_3 with respect to Tx_1, Tx_2 and Tx_3 are chosen for trilateration positioning. The equations for trilateration can be expressed as

$$\begin{cases} {d_1}^2 = (x_1 - x)^2 + (y_1 - y)^2 + (z_1 - z)^2 \\ {d_2}^2 = (x_2 - x)^2 + (y_2 - y)^2 + (z_2 - z)^2 \\ {d_3}^2 = (x_3 - x)^2 + (y_3 - y)^2 + (z_3 - z)^2 \end{cases} \tag{7}$$

where x_j, y_j, z_j, $j = 1, 2, 3$ are the coordinates of the selected three LEDs, which can be obtained using the look-up table based on the subcarrier index. x, y, z are the coordinates of Rx. Suppose $z_1 = z_2 = z_3 = h$, $z = 0$, then $\cos(\varphi_i) = \cos(\phi_i) = h/d_i$, d_i can be calculated as

$$d_i = \begin{cases} \left(\frac{A_r(m+1)T_s G_s h^{m+1}}{2\pi H_i}\right)^{\frac{1}{m+3}}, & 0 \le \phi_i \le \phi_c \\ 0, & \phi_i > \phi_c. \end{cases} \tag{8}$$

H_i can be determined as

$$H_i = Y_i/(R \times A). \tag{9}$$

Therefore, the final estimated d_i can be calculated from

$$d_i = \begin{cases} F \times {Y_i}^E, & 0 \le \phi_i \le \phi_c \\ 0, & \phi_i > \phi_c \end{cases} \tag{10}$$

where F and E are constant coefficient depending on specific subcarrier. Equation (7) can be rewritten as

$$\mathbf{B}X = \mathbf{C} \tag{11}$$

where

$$\mathbf{B} = \begin{bmatrix} x_2 - x_1 & y_2 - y_1 \\ x_3 - x_1 & y_3 - y_1 \end{bmatrix}, \quad \mathrm{X} = \begin{bmatrix} x \\ y \end{bmatrix}$$

$$\mathbf{C} = \begin{bmatrix} ({d_1}^2 - {d_2}^2 + x_2^2 + y_2^2 - x_1^2 - y_1^2)/2 \\ ({d_1}^2 - {d_3}^2 + x_3^2 + y_3^2 - x_1^2 - y_1^2)/2 \end{bmatrix}.$$

The equation can be solved using the linear least square method given by

$$\mathrm{X} = (\mathbf{B}^T\mathbf{B})^{-1}\mathbf{B}^T\mathbf{C}. \tag{12}$$

3. Experiment Setup and Results

The feasibility of the proposed scheme is demonstrated experimentally as shown in Fig. 2. The coordinates of Txs1, 2, and 3 are (7, 7, 15), (7, 14, 15), and (14, 7, 15), respectively, and the Rx with the coordinate of (x, y, 0) is located at the floor level. We have used a total of 128 subcarriers of which 3 are used for positioning and the rest for data transmission, as shown in Fig. 3. The block diagram of OFDM coder and decoder is shown in Fig. 4. At the Tx, the data blocks encoded into quadrature phase shift keying (QPSK) symbols are combined with positioning data prior to being applied to N-point IDFT. The transmitted positioning data $I_1\, I_2\, I_3$ are $(1 + i\ 0\ 0)$, $(0\ 1 + i\ 0)$ and $(0\ 0\ 1 + i)$ for Txs 1, 2 and 3, respectively. In order to mitigate multipath induced intersymbol interference (ISI) between OFDM symbols, the cycle prefix (CP) is inserted at the front of each data block. Training symbols are inserted at the start of each OFDM frame for channel estimation and synchronization. The generated OFDM signal at 1.7 Mbaud is three times up-sampled and then up-converted to 1.25 MHz using digital I-Q modulation, which is then uploaded into an arbitrary waveform generator

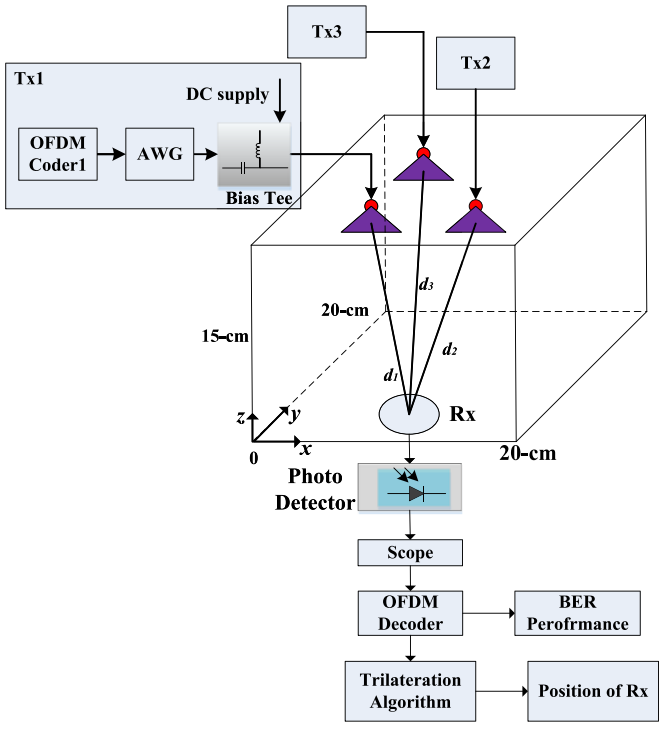

Fig. 2. Experiment setup for OFDMA visible light communications and positioning (Modules shown within Tx1 also apply to Tx2&3).

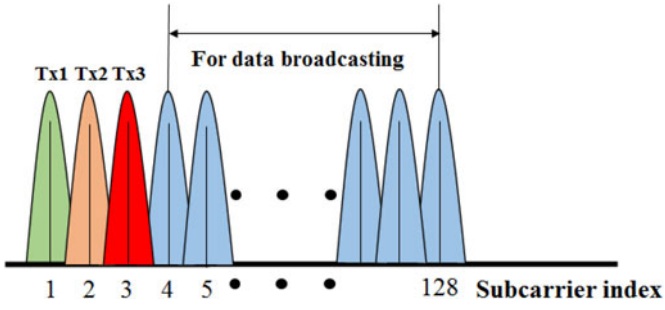

Fig. 3. Subcarrier allocation for positioning and data brocasting.

(AWG) operating at 5-MS/s. The output of AWG (i.e., OFDM signal) with 20 V peak to peak voltage is DC-level shifted using a bias Tee prior to IM of a commercially available phosphorescent white LED. At the Rx, a commercial optical Rx composed of Si photodetector and an amplifier (THORLABS PDA36A) is used to convert the optical signal back into the electrical signal. The optical Rx output is captured using a real-time digital oscilloscope for OFDM demodulation and further signal processing in the Matlab domain. The OFDM decoder functionality is opposite of that of OFDM coder. Following DFT, the positioning data is obtained to calculate the position of Rx using the trilateration algorithm, whereas the broadcasting data is demodulated prior to channel equalization. All the key system parameters are provided in Table 1.

In the proposed scheme, it is very difficult to obtain accurate relationship between the distance and received signal strength (RSS) (i.e., (10)) accuracy. Here, we performed measurements at 16 points with coordinates of (0, 0, 0), (0, 6, 0), (0, 14, 0), (0, 20, 0), (6, 0, 0), (6, 14, 0), (6, 20, 0), (14, 0, 0), (14, 6, 0), (14, 14, 0), (14, 20, 0), (20, 0, 0), (20, 6, 0), (20, 14, 0), and (20, 20, 0). Based on these measured results we calculated the coefficients in (10). Fig. 5 shows the transmission distance as

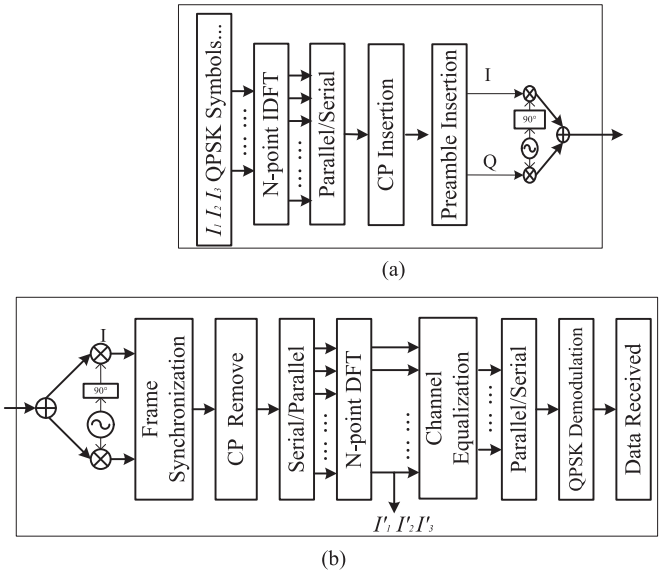

Fig. 4. Block diagram of (a) OFDM coder and (b) OFDM decoder.

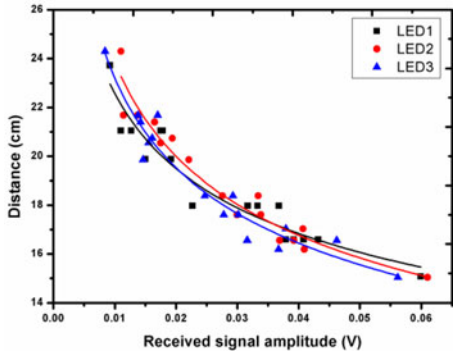

Fig. 5. Distance between Tx and Rx as a function of received signal amplitude.

a function of RSS for LEDs 1, 2, and 3, respectively. By fitting the scatter points, the final estimated d_1, d_2 and d_3 can be written as

$$d_1 = 8.5267 \times Y_1^{-0.21135} \tag{13}$$

$$d_2 = 7.3869 \times Y_2^{-0.2545} \tag{14}$$

$$d_3 = 7.3939 \times Y_3^{-0.2482}. \tag{15}$$

Fig. 6 depicts the estimated as well as reference positions using the proposed scheme. The PE is given by

$$D_{error} = \sqrt{(x - x_e)^2 + (y - y_e)^2} \tag{16}$$

where (x, y) and (x_e, y_e) are the coordinates of reference and estimated points, respectively. Using (16) the mean PE is with 1.68 cm. The positioning accuracy of the proposed scheme depends on the signal to noise ratio (SNR) of the three subcarriers that are employed for localization. Fig. 7 shows the PE as a function of noise power. We suppose the relationship between the distance and RSS can be exactly obtained. A larger noise would cause a bigger PE. The noise following

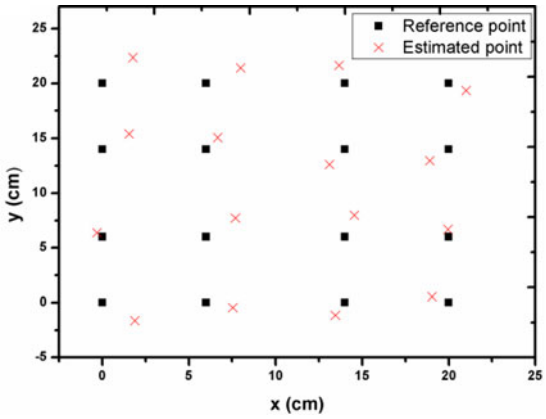

Fig. 6. Final estimated positions using our proposed scheme.

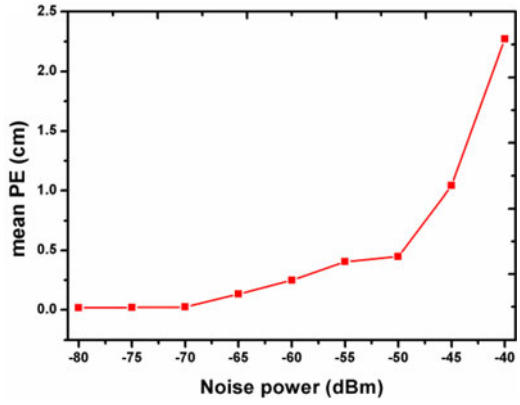

Fig. 7. Positioning error as a function of noise power.

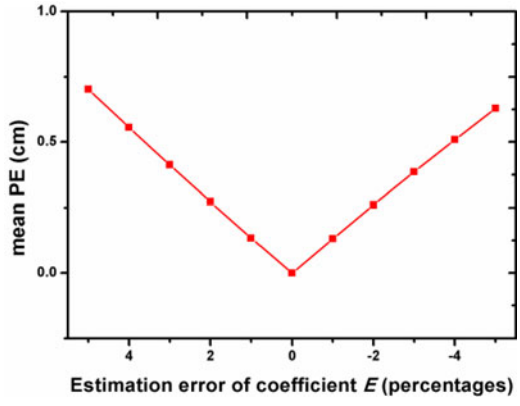

Fig. 8. Positioning error as a function of estimation error for coefficient *E*.

Gaussian distribution not only causes a positioning error but also estimation errors of coefficients. Figs. 8 and 9 show the mean PE as a function of the estimation error percentages for coefficient *E* and *F*, respectively. We assume the SNR is high enough to estimate the distance. As shown in Figs. 8 and 9, the estimation errors of coefficients also cause a PE. The positioning accuracy of the proposed scheme can be improved using high-power LEDs and high-gain optical concentrators to increase the SNR. Moreover, more effective method to calculate the relationship between the distance and RSS should be studied to obtain accurate positioning. To assess the link performance

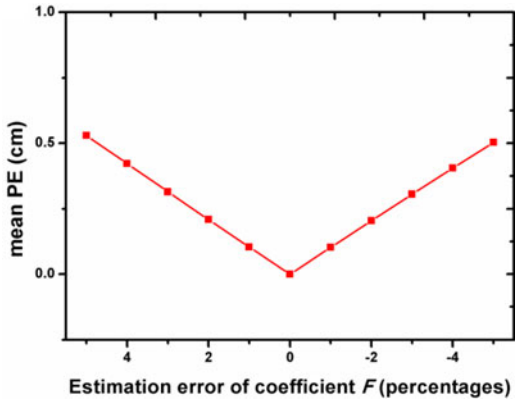

Fig. 9. Positioning error as a function of estimation error for coefficient F.

TABLE 1
System Parameters

Parameter	Value
LED	
• Bandwidth	$<$5 MHz
• Semi-angle of half power $\varphi_{1/2}$	$\sim 60^{o}$
• Transmit power	180 mw
• DC bias	0.8 A
Pin photodetector	
• Active area A_r	13 mm^2
• Responsivity R	$<$0.4 A/W
• Bandwidth	10 MHz
Height	15 cm
FOV of receiver	90^{o}
Gain of optical filter T_s	1
Gain of optical concentrator G_s	1

TABLE 2
EVM Performance for Data Broadcasting

	$x = 0$ cm	$x = 6$ cm	$x = 14$ cm	$x = 20$ cm
$y = 0$ cm	17.5 dB	18.9 dB	18.5 dB	15 dB
$y = 6$ cm	18.7 dB	19.4 dB	17.9 dB	17.1 dB
$y = 14$ cm	17.9 dB	18.5 dB	17.8 dB	17 dB
$y = 20$ cm	17.6 dB	18.6 dB	17.7 dB	15 dB

we have measured the EVM [14] as displayed in Table 2, where an EVM of more than 15 dB at each measured point is acquired for data broadcasting.

4. Conclusion

In this paper, we proposed a new VLC based indoor positioning system. To overcome the intercell interference, the OFDMA scheme was employed. The experiment results showed that the proposed indoor positioning method could readily overcome the intercell interference, and provide both indoor positioning and data communications. We showed that the proposed system with QPSK offered a mean positioning error and an error vector magnitude (EVM) of 1.68 cm and more than 15 dB, respectively. The OFDMA-VLC positioning systems provide high spectral efficiency, high tolerance against multipath-induced distortion and flexible bandwidth allocation. The positioning accuracy of the proposed scheme depended on the SNR of received OFDM signal and the estimation accuracy of distance, which could be improved using high-power LEDs and high-gain optical concentrators. In addition, more effective method to calculate the relationship between the distance and RSS should be studied to obtain accurate positioning.

References

[1] X. H. Liu, H. Makino, and Y. Maeda, "Basic study on indoor location estimation using visible light communication platform," in *Proc. IEEE 30th Annu. Int. Eng. Med. Biol. Soc.*, Vancouver, BC, Canada, Aug. 2008, pp. 2377–2380.
[2] H. Elgala, R. Mesleh, and H. Haas, "Indoor optical wireless communication: Potential and state-of-the-art," *IEEE Commun. Mag.*, vol. 49, no. 9, pp. 56–62, Sep. 2011.
[3] Y. U. Lee, S. Baang, J. Park, Z. Zhou, and M. Kavehrad, "Hybrid positioning with lighting LEDs and Zigbee multihop wireless network," *Proc. SPIE*, vol. 8282, pp. 16–22, Jan. 2012.
[4] A. Papapostolou and H. Chaouchi, "Scene analysis indoor positioning enhancements," *Annals Telecommun.*, vol. 66, no. 9–10, pp. 519–533, Oct. 2011.
[5] M. G. Moon and S. I. Choi, "Indoor position estimation using image sensor based on VLC," in *Proc. Int. Conf. IEEE Adv. Technol. Commun.*, 2014, pp. 11–14.
[6] H. Kim, D. Kim, S. Yang, Y. Son, and S. Han, "An indoor visible light communication positioning system using a RF carrier allocation technique," *J. Lightw. Technol.*, vol. 31, no. 1, pp. 134–144, Jan. 2013.
[7] S. Yang, D. Kim, H. Kim, Y. Son, and S. Han, "Visible light based high accuracy indoor localization using the extinction ratio distributions of light signals," *Microw. Opt. Technol. Lett.*, vol. 55, no. 6, pp. 1385–1389, 2013.
[8] S. Yang, H. Kim, Y. Son, and S. Han, "Reduction of optical interference by wavelength filtering in RGB-LED based indoor VLC system," in *Proc. IEEE Opto-Electron. Commun. Conf.*, 2011, pp. 551–552.
[9] Y. Hou, S. Xiao, H. Zheng, and W. Hu, "Multiple access scheme based on block encoding time division multiplexing in an indoor positioning system using visible light," *J. Opt. Commun. Netw.*, vol. 7, no. 5, pp. 489–495, May 2015.
[10] H. S. Kim D.-H. Kwon, S.-H. Yang, Y.-H. Son, and S.-K. Han, "Channel assignment technique for RF frequency reuse in CA-VLC based accurate optical indoor localization," *J. Lightw. Technol.*, vol. 32, no. 14, pp. 2544–2555, Jul. 2014.
[11] T. Komine and M. Nakagawa, "Fundamental analysis for visible light communication system using LED lights," *IEEE Trans. Consum. Electron.*, vol. 50, no. 1, pp. 100–107, Feb. 2004.
[12] P. Chvojka, S. Zvanovec, P. A. Haigh, and Z. Ghassemlooy, "Channel characteristics of visible light communications within dynamic indoor environment," *J. Lightw. Technol.*, vol. 33, no. 9, pp. 1719–1725, May 1, 2015.
[13] A. Burton, H. Le-Minh, Z. Ghassemlooy, S. Rajbhandari, and P. A. Haigh, "Smart receiver for visible light communications: Design and analysis," in *Proc. 8th Int. Symp. Commun. Syst., Netw. Digit. Signal Process.*, Jul. 18–20, 2012, pp. 1–5.
[14] R. Schmogrow *et al.*, "Error vector magnitude as a performance measure for advanced modulation formats," *IEEE Photon. Technol. Lett.* vol. 24, no. 1, pp. 61–63, Jan. 2012.